

Comparative Analysis of Hybrid Controllers of Done Systems (UPFC) and Interphase Power Regulators Type RPI 30p15 on Contingency Management in Electrical Networks

Koko Koko Joseph¹, Nneme Nneme Léandre¹, Ndjakomo Essiane Salomé²,
Batassou Guilzia Jeannot¹

¹Laboratory of Computer and Automatic Engineering, UFD of Engineering Sciences, ENSET, University of Douala, Douala, Cameroon

²Higher Normal School of Technical Education ENSET of EBOLOWA, University of Yaoundé 1, Yaoundé, Cameroon

Email: kokojoseph469@yahoo.fr, leandren@gmail.com, salomendjakomo@gmail.com, batassoujeannot@yahoo.fr

How to cite this paper: Joseph, K.K., Léandre, N.N., Salomé, N.E. and Jeannot, B.G. (2021) Comparative Analysis of Hybrid Controllers of Done Systems (UPFC) and Interphase Power Regulators Type RPI 30p15 on Contingency Management in Electrical Networks. *World Journal of Engineering and Technology*, 9, 708-726.

<https://doi.org/10.4236/wjet.2021.93048>

Received: April 15, 2021

Accepted: August 28, 2021

Published: August 31, 2021

Copyright © 2021 by author(s) and Scientific Research Publishing Inc. This work is licensed under the Creative Commons Attribution International License (CC BY 4.0).

<http://creativecommons.org/licenses/by/4.0/>



Open Access

Abstract

The aim of this work is to demonstrate that interphase power regulators (IPR) bring new and interesting ultra-solutions that complement those already taken into account by the FACTS (Flexible Alternative Transmission System) in the resolution of the problems related to the power flow in the AC transmission networks. In order to facilitate the understanding of this work, a comparative study of the performances of the two technologies between the UPFC (Unified Power Flow Controller) and RPI was carried out and at the end of which we were able to highlight the preponderance of RPI compared to the UPFC in the bypassing of the short-circuit fault insofar as the latter allows, in particular, an increase in the transformation capacity without an increase in the level of the short-circuit. The decoupled watt-var method has been used to control the UPFC while the RPI is controlled by phase shift. The simulation results are obtained in the Matlab Simulink environment and show the flexibility of the RPI compared to the UPFC in limiting strong contingencies.

Keywords

Transmission Line, High Contingency, FACTS, PST, TCPST, UPFC, Three-Leg RPI 30P15, Phase-Shifting Transformer, Modeling

1. Introduction

Nowadays, the problems related to the operation of the production, transmission and distribution networks of electrical energy have taken a considerable magnitude. Like any productive sector, the production and transmission of energy are

subject to the laws of a constantly growing market. In addition to the deregulation of the development of interconnections and the fluctuations of fuel prices, the economic aspect forces operators to manage the existing (generation sources, transmission lines, etc.) in the most profitable way possible [1]. However, the management of the power produced and transmitted through the network is not the only concern of the operators. This is all the more true since, in addition to the stochastic variations linked to non-linear and dynamic loads, severe faults with devastating effects (short-circuit, overvoltage, loss of an important production unit...etc.) can occur and plunge the network out of its stable operating regime. In addition, improving quality and reducing operating costs while respecting the constraints of the network, are considered as major issues of power flow. Facing such remarkable requirements, the use of active lines is considered. In the sense they can react almost instantaneously to a contingency and counteract a potentially dangerous situation [2]. In order to respond favorably to this problem, several research works have been carried out and have brought a considerable push in the improvement of power transit and particularly the advancement of the technology of flexible AC transmission systems and interphase power regulators. However, FACTS devices present some malfunctions in the face of a certain short circuit peak. The need to create new power flow controllers to overcome the limitations of network operation caused by high short-circuit levels was the main motivation that in 1997 led JACQUES BROCHU [3] to present a thesis entitled "Interphase power controllers in steady state" in which he addresses the issue of adapting IPR technology to certain network problems, through the description of three applications that, to date, have proven to be more promising both technically and economically. The concern is to highlight the preponderance of each technology over the other in various contexts of power line operation.

2. Materials and Methods

2.1. Materials

2.1.1. Hypothesis

To carry out our work, we made the following considerations: the generator and switches of our converter on the one hand and the phase-shifting transformer on the other hand will be assumed ideal, the line balanced, the voltage drops across the line represented by the reactance X , the inductance of the line is represented by L . The characteristics of the line are given in the **Table 1**.

Table 1. Characteristics of the studied line [3].

U (KV)	F (HZ)	L (km)	R (ohm)	X (ohm)	P (MW)	Q (MVAR)
500	60	200	14.77	69.72	1120	840
S (MVA)						1400
φ (°)						36.869

2.1.2. Case of UPFC

The block diagram of the UPFC is given in **Figure 1**, which will be used to model this device in the matlab-simulink environment.

Applying Kirchhoff's laws [4] to the meshes of the circuit in **Figure 1** gives us the mathematical equations governing our system as follows:

$$\begin{cases} V_{sa} - V_{ca} - V_{ra} = r i_{sa} + L \frac{di_{sa}}{dt} \\ V_{sb} - V_{cb} - V_{rb} = r i_{sb} + L \frac{di_{sb}}{dt} \\ V_{sc} - V_{cc} - V_{rc} = r i_{sc} + L_p \frac{di_{sc}}{dt} \end{cases} \quad (1)$$

In order to minimize the computing time, we have switched from the three-phase system to the two-phase system, *i.e.* from three-phase reference frames with coordinates a, b and c, to two-phase reference frames with coordinates d and q. The transformation matrix is the following (Park's matrix) [5]:

$$K = \sqrt{\frac{2}{3}} \begin{bmatrix} \cos wt & \cos\left(wt - \frac{2\pi}{3}\right) & \cos\left(wt + \frac{2\pi}{3}\right) \\ \sin wt & \sin\left(wt - \frac{2\pi}{3}\right) & \sin\left(wt + \frac{2\pi}{3}\right) \\ \frac{1}{\sqrt{2}} & \frac{1}{\sqrt{2}} & \frac{1}{\sqrt{2}} \end{bmatrix} \quad (2)$$

So the system becomes:

$$\begin{cases} V_{psd} - V_{cd} - V_{rd} = r i_{psd} + L \frac{di_{sd}}{dt} - wL i_q \\ V_{sq} - V_{cq} - V_{rq} = r i_{sq} + L \frac{di_{sq}}{dt} + wL i_d \end{cases} \quad (3)$$

Using the matrix representation on the system we have:

$$\frac{d}{dt} \begin{bmatrix} i_{sd} \\ i_{sq} \end{bmatrix} = \begin{bmatrix} \frac{-r}{L} & w \\ -w & \frac{-r}{L} \end{bmatrix} \cdot \begin{bmatrix} i_{sd} \\ i_{sq} \end{bmatrix} + \frac{1}{L} \cdot \begin{bmatrix} V_{sd} - V_{cd} - V_{rd} \\ V_{sq} - V_{cq} - V_{rq} \end{bmatrix} \quad (4)$$

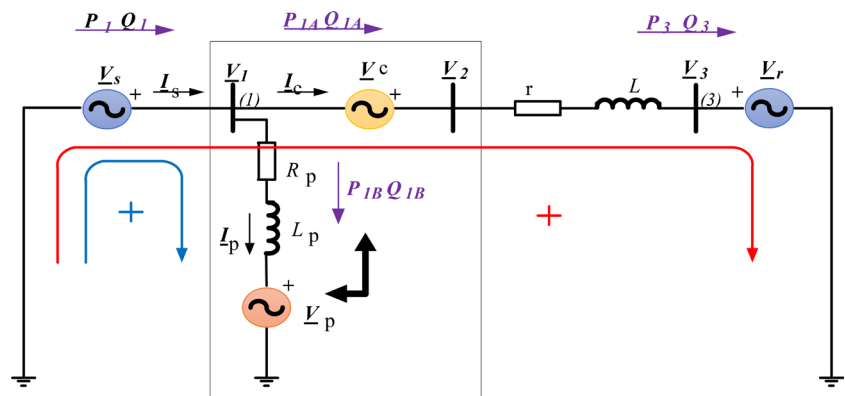


Figure 1. Physical representation of a UPFC converter connected to the network for modeling purposes.

The equation above corresponds to our model of serial converter. It will be used to build, under Simulink, the block which represents the serial part of the system. We also want to remind that the principle applied on the serial part will be the same on the parallel part of our system.

2.1.3. Case of RPI 30P15

The interphase power regulator uses a group of three-phase inductors and capacitors each installed in series between two networks or subnetworks. What distinguishes this new class of equipment from other series compensation equipment is the way the series components are connected to the networks. For example, the A-phase inductor and capacitor of the first network could be connected to the B and C phases of the network. When all the components are energized, the magnitude and phase angle (δ) of the current is set in one of the two buses to which the controller is connected. The current control thus allows the power carried by the controller to be adjusted, as well as the reactive power absorbed or generated at one of the buses. Inductors and capacitors are always considered perfect without losses. The impedances of the series components are then reduced to their imaginary part, *i.e.* the reactance. In the context of the controller where the series components are arranged in parallel to each other, the term susceptance is used instead of reactance for practical reasons ($B = -1/X$) [6]. (Figure 2)

RPI technology has given rise to a wide range of devices that can take many different forms depending on the application. Before entering fully into the description of RPI, we felt it necessary to take a look at a few examples in order to highlight the versatility of the technology as well as the need for the analytical means presented later. Table 2 presents the main characteristics of the RPI topologies.

- Number of branches

The number of branches in an RPI is one of its most fundamental aspects. In general, the single-phase. In general, the single-phase circuit of an RPI can have n branches in parallel. In practice, however, this number is kept to a minimum in order to limit the size and cost of the device. It is the angular range of the angle δ_{sr} across the device that defines the number of branches. [7]

- Types of interphase power regulators

Depending on the connection bar, there are two types of interphase power controllers: synchronous interphase power controllers and asynchronous interphase power controllers.

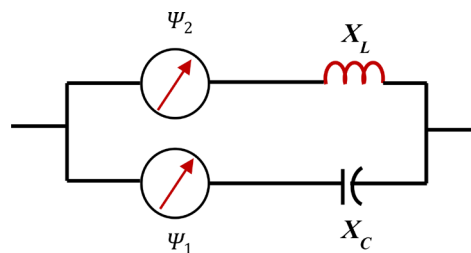


Figure 2. Diagram RPI connected between two networks or subnets [7].

To illustrate this, and at the same time justify the construction constraints that we will use later, the configuration of RPI highlighted in our work is the one with a phase-shifting transformer (PST) in parallel with a capacitor; it is the RPI 30P15. This configuration is illustrated in **Figure 3**.

The model of our RPI connected to the network can be related to a quadropole as shown in **Figure 4**.

The power balance of this circuit leads to the following equations.

- Sign convention of the powers.

Table 2. Topological characteristics of the RPI [8].

Topology	A number of branches	Nature of branches	Phase shift method	angle δ_{ar} (degré)	Adjustment method
	240		Connexion	240	
	180			180	susceptance
	120		transformation	120	
Synchronous	30P1530M15	2	Simple (C or L)	30	
	60 with 90° injection			0 à 60	phase shift
	20with variable injection			0 à 20	Phase shift and transformation ratio
Asynchronous	3 branches	3		120	susceptance
	4 branches	4	Double (C and L) transformation	90	
	4 branches and shunting	4			

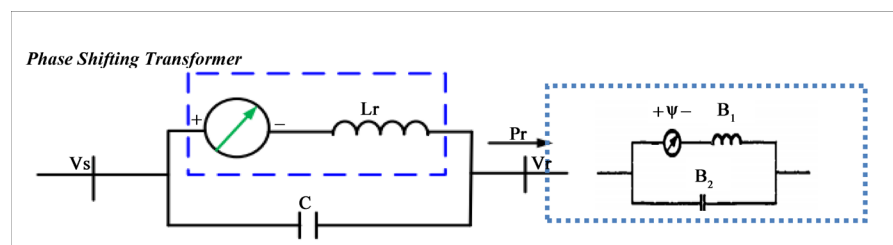


Figure 3. RPI carried out by means of a transformer-phase-converter and of a condenser [9].

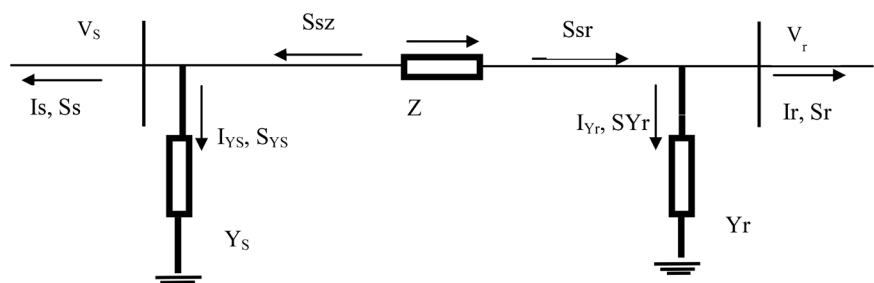


Figure 4. Quadropole in π [10]

The apparent powers S_s and S_r are defined in the same direction as the currents.

While posing:

$$V_s = V_s e^{j\delta_{B1}} \quad (5)$$

$$V_r = V_r e^{j\delta_{B2}} \quad (6)$$

$$\begin{cases} \delta_{B1} = \delta - \phi_1 \\ \delta_{B2} = \delta - \phi_2 \end{cases} \quad (7)$$

While for the powers S_r and S_s of the shunt admittances we obtain:

$$S_s = \frac{V_s V_r e^{j\delta_{B1}}}{Z^*} - \frac{V_s^2}{Z^*} \quad (8)$$

$$S_r = \frac{V_s V_r e^{j\delta_{B2}}}{Z^*} - \frac{V_r^2}{Z^*} \quad (9)$$

These power equations are based on the following assumptions: The system is symmetrical, so it is always possible to represent a three-phase element by a single-phase equivalent; the frequencies of the S and R bars are essentially the same ($f_s = f_r$), so that it is possible to use the phasors for the equation; the series elements are linear (they do not produce harmonics).

While posing:

$$Z = R + jX \quad (10)$$

$$\underline{Y}_s = G_s + jB_s \quad (11)$$

$$\underline{Y}_r = G_r + jB_r \quad (12)$$

We can rewrite as am in trigonometric form

$$\begin{aligned} \underline{S}_s &= \frac{1}{Z} [V_s V_r R \cos(\delta_{B1}) - X \sin(\delta_{B1}) - V_s^2 R] \\ &+ \frac{1}{Z} [V_s V_r R \sin(\delta_{B1}) + X \cos(\delta_{B1}) - V_s^2 R] \end{aligned} \quad (13)$$

$$\begin{aligned} \underline{S}_r &= \frac{1}{Z} [V_s V_r R \cos(\delta_{B2}) - X \sin(\delta_{B2}) - V_r^2 R] \\ &+ \frac{1}{Z} [V_s V_r R \sin(\delta_{B2}) + X \cos(\delta_{B2}) - V_r^2 R] \end{aligned} \quad (14)$$

$$\underline{S}_s = V_s^2 (G - jB_1) = -P + jQ_s \quad (15)$$

$$\underline{S}_r = V_r^2 (G - jB_2) = P + jQ_r \quad (16)$$

The active power P is positive when the power flow occurs from the S side to the right side, the reactive power Q_s and Q_r are positive when the IPC generates reactive power to the buses to which it is connected Since $\delta_{B1} = -\delta_{B2}$ the powers P , Q_s and Q_r of the series element, formulas in terms of conductance and susceptance, become in matrix form [11]:

$$\begin{bmatrix} -V_s V_r \sin \delta_{B1} & -V_s V_r \sin \delta_{B2} \\ V_s^2 - V_s V_r \cos \delta_{B1} & V_s^2 - V_s V_r \cos \delta_{B2} \\ V_r^2 - V_s V_r \cos \delta_{B1} & V_r^2 - V_s V_r \cos \delta_{B2} \end{bmatrix} \begin{bmatrix} B_1 \\ B_2 \end{bmatrix} = \begin{bmatrix} P \\ Q_s \\ Q_r \end{bmatrix} \quad (17)$$

$$B_1 = \frac{P(2V_r - V_s \cos \delta - \sqrt{3}V_s \sin \delta) - Q_r V_r (\sqrt{3} \cos \delta - \sin \delta)}{\sqrt{3}V_s V_r (V_s - 2V_r \cos \delta)} \quad (18)$$

$$B_2 = \frac{-P(2V_r - V_s \cos \delta + \sqrt{3}V_s \sin \delta) - Q_r V_r (\sqrt{3} \cos \delta + \sin \delta)}{\sqrt{3}V_s V_r (V_s - 2V_r \cos \delta)} \quad (19)$$

Equations two and three of (3.15) indicate that the reactive powers are coupled to each other by the following simple Orelation:

$$Q_s = (B_1 + B_2)(V_s^2 - V_r^2) + Q_r \quad (20)$$

Figure 5 below illustrates the three-phase model of our RPI on a three-phase network.

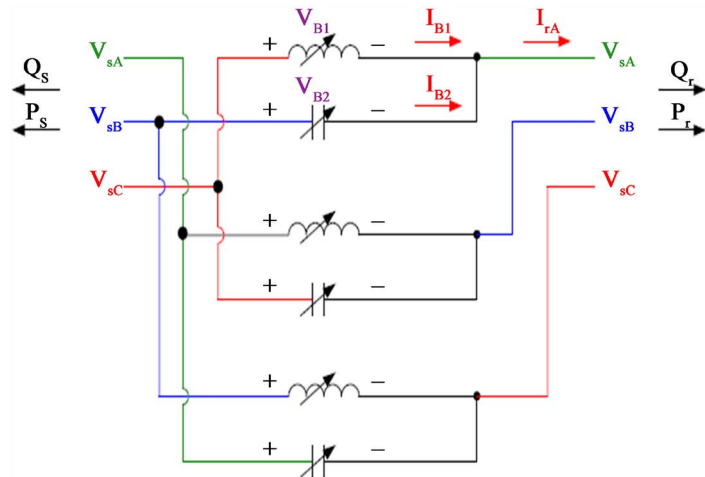


Figure 5. three-phase model of the RPI30P15 connecting two regions of a network [12].

3. Methods

3.1. Case of UPFC

Theoretically, the UPFC should be treated as a multivariable system because the two series and parallel converters are connected on one side to the transmission line and on the other side to the DC circuit and therefore have two outputs each [13]. Therefore, in order to facilitate the synthesis of the controllers, the processing of the two converters will be done separately. There are several possible configurations for controlling this compensator. But first we must determine the references to control the device. There are several methods of identifying the references (control quantities): Method based on the principle of active current, Decoupled Watt-Var Method and the Method of real and imaginary instantaneous power. In this work we have adopted the decoupled watt-var method [14]. The idea of this method comes from the equations of the voltages obtained after the Park transformation. The problem of non-linearity is avoided in this method by considering only the fundamental quantities for the control of our system. (**Figure 6**)

The principle of this method is to transform the measured quantities of cur-

rent and voltage of the three phases on the two d-q axes using the Park transformation. Then the values of the active and reactive powers are imposed and the reference currents are calculated from these values (desired powers) and the values of the voltages measured by the two following equations:

$$i_{sd}^* = \frac{2}{3} \cdot \frac{(p_s^* V_{sd} - q_s^* V_{sq})}{V_{sd}^2 + V_{sq}^2} \quad (21)$$

$$i_{sq}^* = \frac{2}{3} \cdot \frac{(p_s^* V_{sq} + q_s^* V_{sd})}{V_{sd}^2 + V_{sq}^2} \quad (22)$$

Figure 7 below illustrates the control circuit of the UPFC

3.2. Case of RPI

As part of our work, the choice was made on the control technique by variation of phase shift. The choice made on this method was inspired by studies carried out at CITEQ (Beauregard, Brochu, Morinet Pelletier, 1994) showing, however, that the phase-shift variation approach is clearly more interesting both in terms of performance and costs. Thyristor Controlled Phase Shift Transformer is a device based on phase shift and thyristor transformer technologies. PSTs are transformers with a complex transformation ratio. These transformers as a power flow controller, reduce transmission losses. With the advancement of power electronics devices, mechanical tap changers are replaced by thyristors, increasing the speed of phase shifters. The phase angle difference between the terminals of the TCPST is absorbed by a series transformer (step-up transformer) with a transmission line. The power budget of an RPI connected to the grid shows that it is possible to regulate the transit of active and reactive power between two systems, either by adjusting the amplitudes of the voltages or the angle of transport between the lines. This is what the phase-shifting transformer does. According to these equations if the voltages V_s and V_r are of the same amplitude, the power transit between the two points can be ensured by a variation of the angle between the two

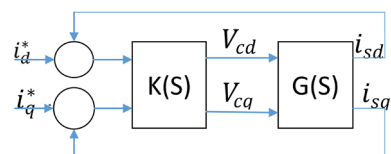


Figure 6. Control circuit of the UPFC [8].

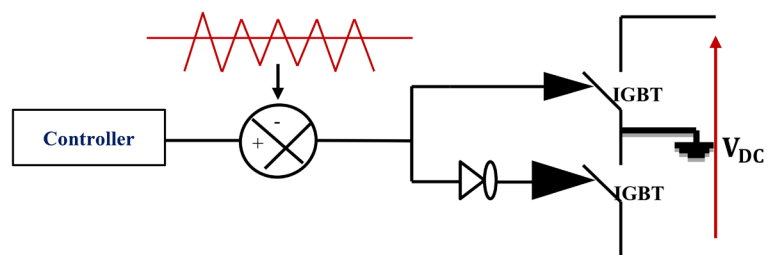


Figure 7. Principle of the PWM Sinus-Triangle command [15].

points using a symmetrical phase-shifting transformer [16]. The equations become [17]:

$$P = \frac{3|V_1^2|}{X + X_{TD}} \sin(\delta \pm \alpha) \tag{23}$$

$$Q = \frac{3(|V_1^2| \cos(\delta \pm \alpha) - |V_1^2|)}{X + X_{TD}} \tag{24}$$

where $V_1 = V_2$, X_{TD} is the reactance of the phase-shifting transformer and α is the phase shift introduced by the phase-shifting transformer.

4. Results and Discussion

This part constitutes the heart of our work insofar as it allows us to make a quantitative and qualitative study on the damage caused by any contingency as well as the capacity of bypassing it by the protection device set up. In this work, two types of faults have been studied: the short-circuit fault and the loss of a phase. It is in this sense that we began by bringing out the complete model of our line in the Matlab Simulink environment as represented in **Figure 8**.

This network will therefore be subjected to various tests and at the end of each test a comparative study of the measured quantities will be made. We would also like to remind you that the quantities measured in this work are voltages and currents.

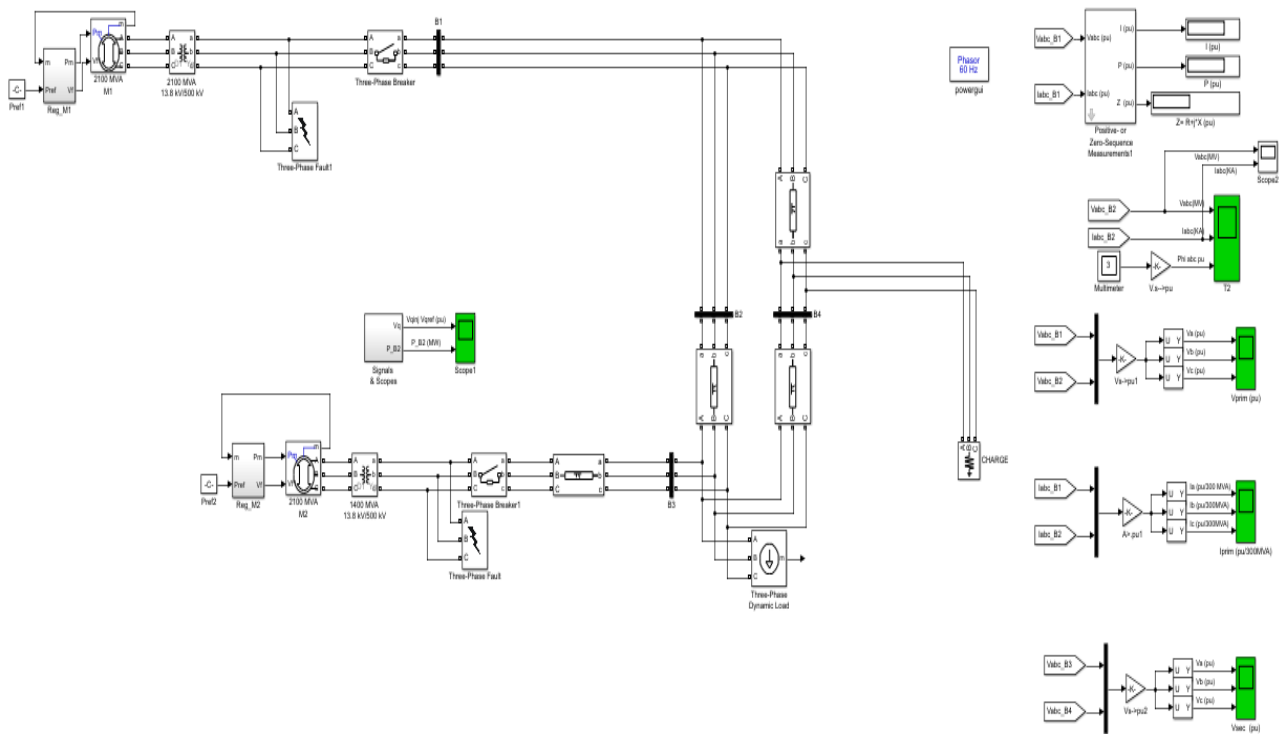


Figure 8. Network without controller.

4.1. Simulation of the Undisturbed Network

During the pre-fault phase, the network is usually in a stable steady state. This phase of network operation is characterized by synchronization of network parameters, such as harmonization of voltages and currents which equalize tan in amplitude and in frequency and shifted by 120 degrees as shown in **Figure 9**.

As soon as a disturbance occurs, the network enters into fault conditions which are very often characterized by a difference between the electrical power of the line and the mechanical power, this difference will be felt on the size of the line as we can see in **Figure 10**.

Figure 10 shows the short circuit that we administered at time $t = 0$ s and which lasted 0.2 ms. We can notice here the difference of amplitude between the phases of none tend to gain while others also lose, can we note that after the phase of operation in the conditions of defect. The network remains unstable, which may cause the opening of the protection devices, resulting in a service interruption. **Table 3** below shows the differences that appear on the network

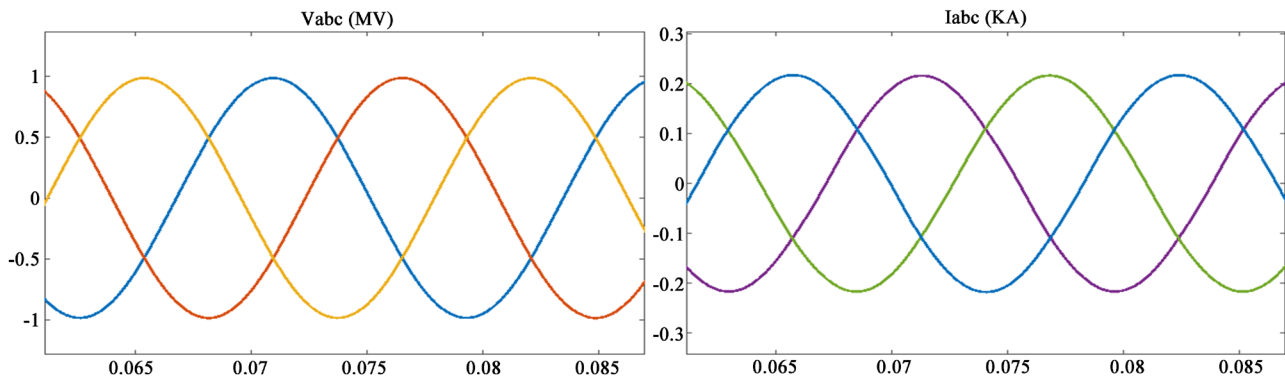


Figure 9. Voltage and current of the fault-free line.

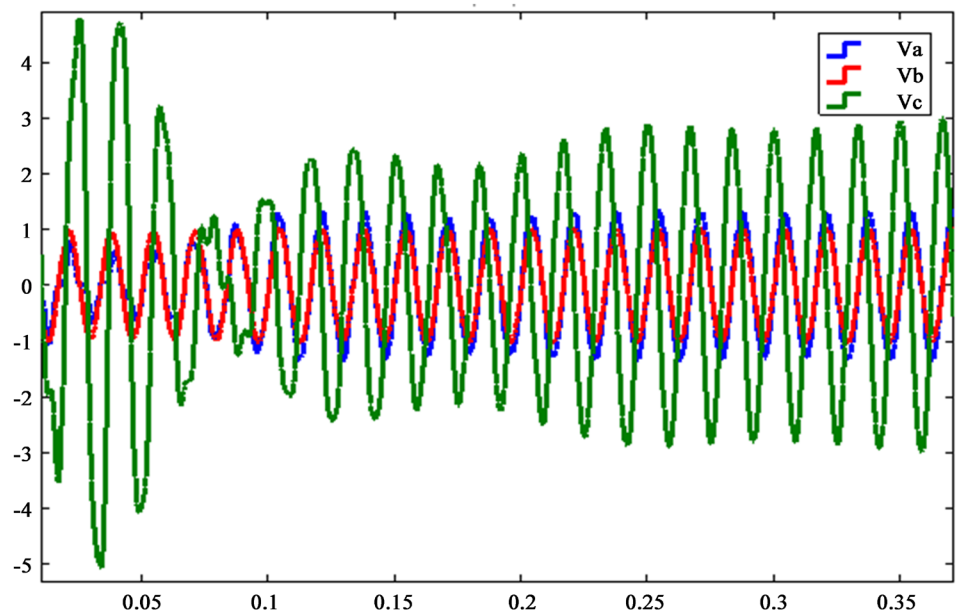


Figure 10. Line voltage and current with fault without controller.

in the presence of this contingency.

Although the system in this case is not severely disturbed, its stability is still critical. In the absence of the control, the system underwent inadmissible oscillations of the transport angle (up to 75 degrees). In this case the network tends to instability, the course of the various parameters of the network is undamped oscillatory (instability of several oscillations), and this is caused by the loss of the equality production-consumption.

4.2. Simulation of the Defect in the Presence of the UPFC Controller

The network assembly plus UPFC is shown below: (Figure 11).

4.2.1. Single-Phase Short-Circuit in the Presence of the UPFC

The short-circuit administered at this level is a short-circuit between phase and neutral, we administered it at the instant $t = 0.05$ ms and which lasted 0.2 ms, the observed behavior is as follows: (Figure 12).

- Visualization of voltages and currents

A single-phase short circuit of 0.2 ms duration in the presence of the UPFC controller gives rise to a transient of 0.12 ms duration with variations as shown in Table 4.

Table 3. Summary of the network without regulator

FAULT NETWORK STATE WITHOUT CONTROLLER						
Sizes	Before defect	In the presence of the defect	Td (ms)	Before defect	Relative error	Relative error in %
φ	36.86	75		0	38.13	103.44
V (MV)	500	265.54	0.2	0	234.46	46.892
I (KA)	2.8	5.69		0	2.89	103.214

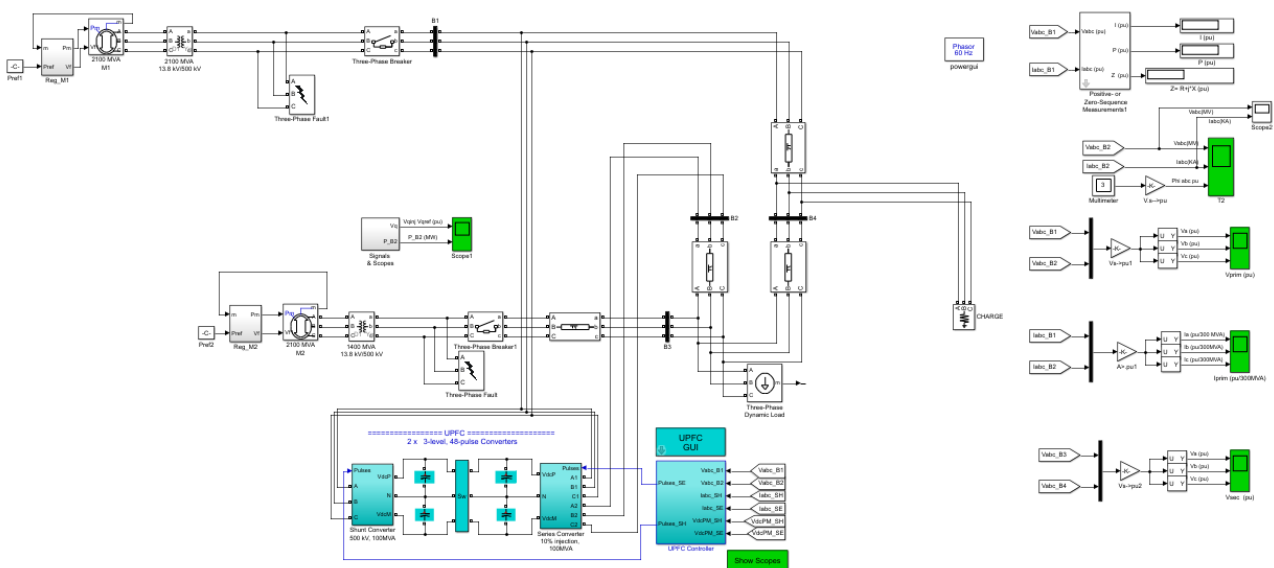


Figure 11. Faulty network in the presence of the UPFC controller.

We notice in this table that a single-phase short-circuit in a network in the presence of the UPFC controller is characterized by a strong increase of the current which tends to exceed the nominal intensity of the line. On the other hand, the opposite is true for the voltages, which forces us to say that the UPFC favors a good maintenance of the voltage plan profile.

4.2.2. Two-Phase Short-Circuit in the Presence of the UPFC

The short-circuit administered at this level is a short-circuit between phase and phase, we have always administered it at the same period $t = 0.05$ ms and for the same 0.2 ms fault duration the observed behavior is as follows: (Figure 13).

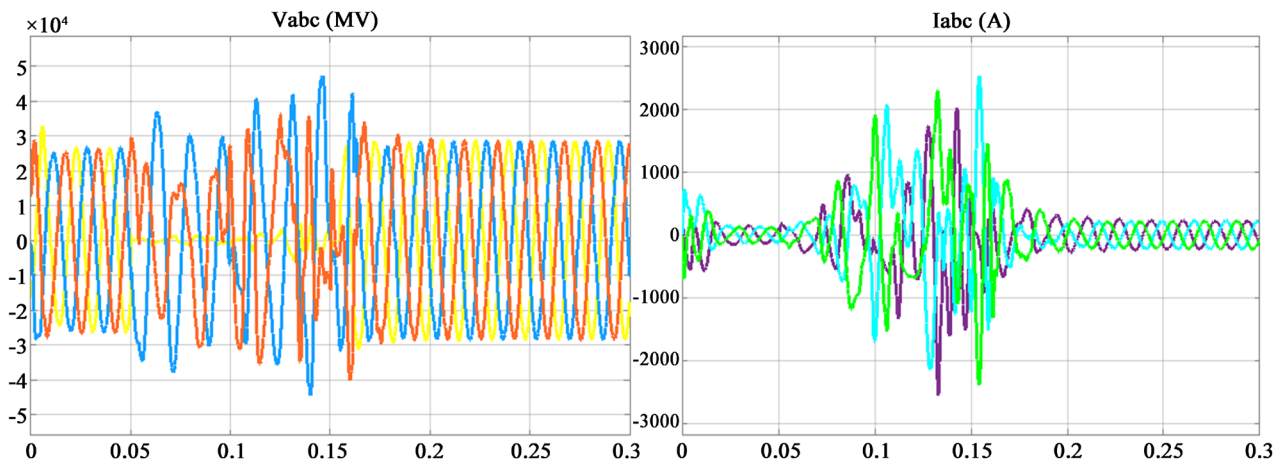


Figure 12. Variation of voltages and currents of a single-phase short-circuited network with UPFC.

Table 4. Variation of single-phase short-circuit network quantities with UPFC.

STATE OF THE NETWORK AT FAULT WITH CONTROLLER						
Nature of the defect		Two-phase short-circuit				
Type of controller	Sizes	Before defect	In the presence of the defect	Td (ms)	Error	Relative error in %
UPFC	V (KV)	500	450	0.2	50	10
	I (KA)	2.8	2.4			

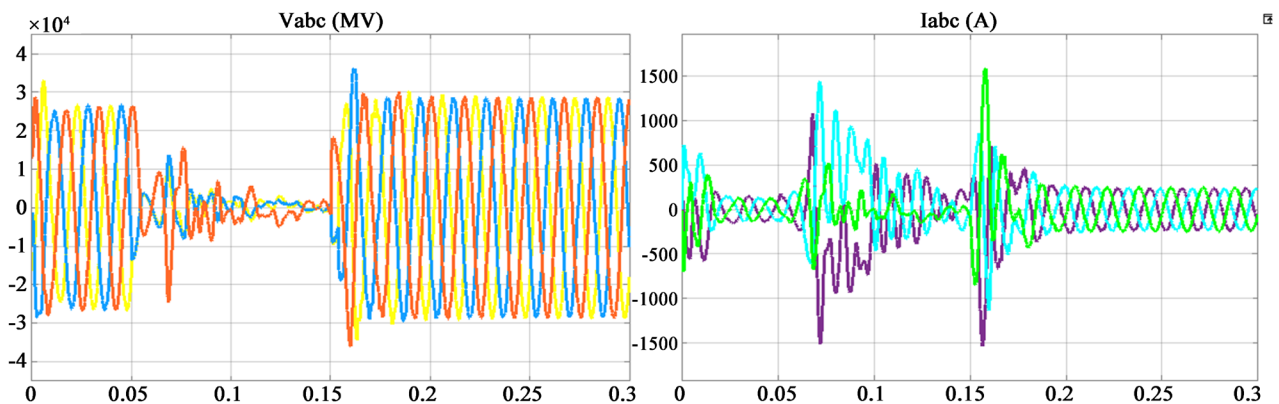


Figure 13. Variation of voltages and currents of a two-phase short-circuited network with UPFC.

- Visualization of voltages and currents

A two-phase short-circuit lasting 0.2 ms in the presence of the UPFC controller gives rise to a transient regime lasting 0.24 ms. **Table 5** below provides information on the evolution of the network parameters in the presence of this fault.

The observation remains the same as for the single-phase short circuit.

4.2.3. Rupture of a Phase in the Presence of UPFC

In this part, we have made the same considerations for the time of the beginning of the fault as for its duration. The loss of one phase of the line in the presence of a controller can generate the phenomena observed below: (**Figure 14**).

- Visualization of voltages and currents

We notice how the appearance of a fault in the presence of the UPFC makes all the phases oscillate and some time later, the network finds a new regime of stable functioning, the oscillations generated by the disturbance disappear with an attenuated amplitude. This during in spite of the presence of the UPFC, the peaks of intensity remain a concern in this network. **Table 6** below shows the evolution of the network parameters in the presence of this fault.

4.2.4. Simulation of Defect in the Presence of Controller RPI

In this section, we are only interested in the disturbed regime of the network in the presence of the RPI controller while considering the results before, in the presence of the fault without unchanged controller. The network plus RPI controller

Table 5. variation of the two-phase short-circuit network quantities with UPFC.

STATE OF THE NETWORK AT FAULT WITH CONTROLLER						
Nature of the defect		Two-phase short-circuit				
Type of controller	Sizes	Before defect	In the presence of the defect	Td (ms)	Error	Relative error in %
UPFC	V (KV)	500	175	0.2	325	65
	I (KA)	2.8	1.63		1.17	41.78

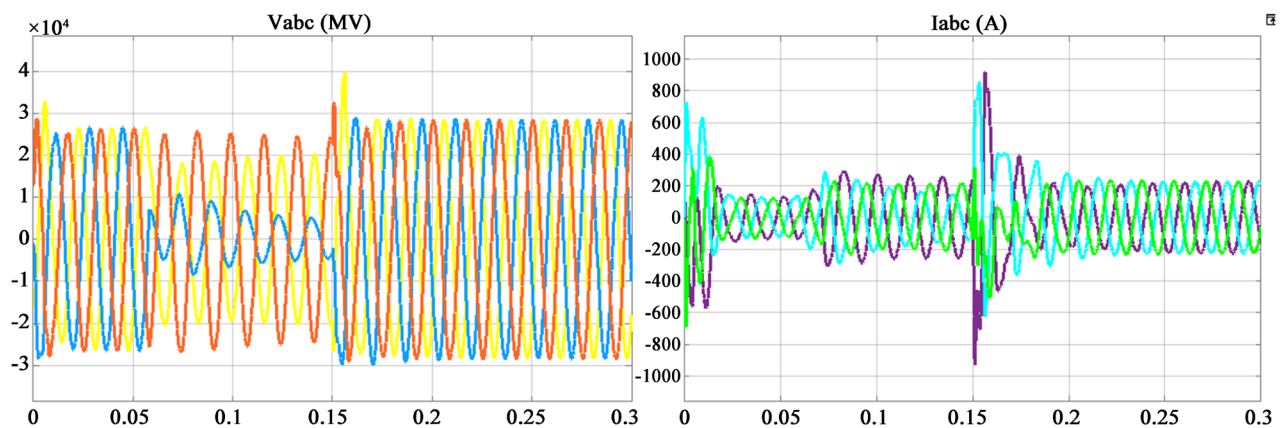


Figure 14. Variation of voltages and currents in a network with a phase deficit with UPFC.

set is represented as follows: (Figure 15).

4.2.5. Single-Phase Short-Circuit in the Presence of the RPI

The short-circuit administered at this level is a short-circuit between phase and neutral, we administered it at the instant $t = 0.05$ ms and which lasted 0.2 ms, the observed behavior is as follows: (Figure 16).

- Visualization of voltages and currents in the presence of an RPI

Table 6. Variation of network quantities in phase failure with UPFC.

STATE OF THE NETWORK AT FAULT WITH CONTROLLER						
Nature of the defect		Rupture of a phase				
Type of controller	Sizes	Before defect	In the presence of the defect	Td (ms)	Error	Relative error in %
UPFC	V (KV)	500	230	0.2	270	54
	I (KA)	2.8	0.9		1.9	90

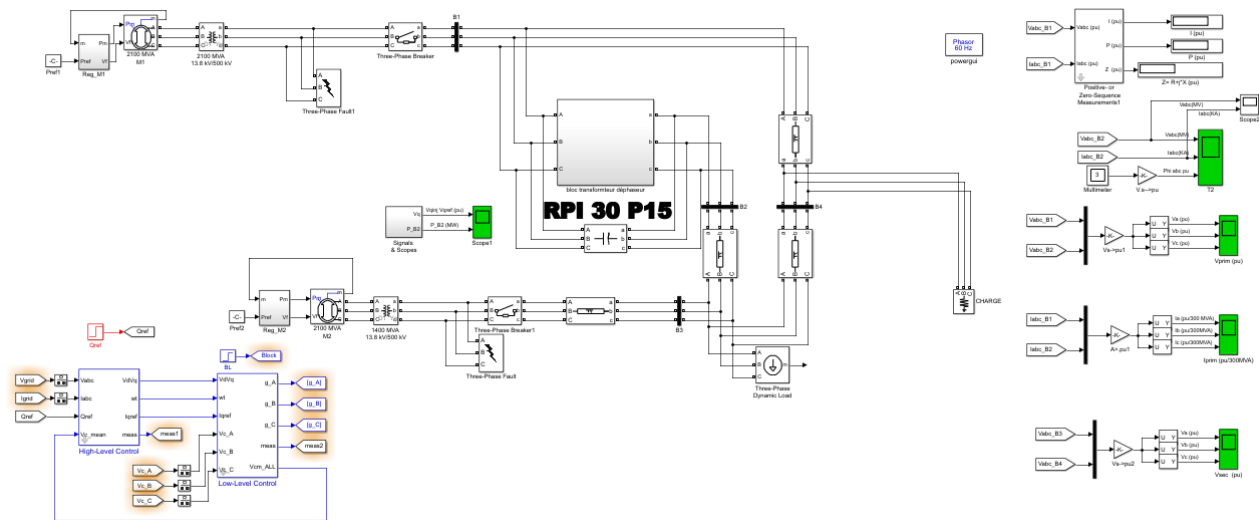


Figure 15. faulty network in the presence of the RPI controller.

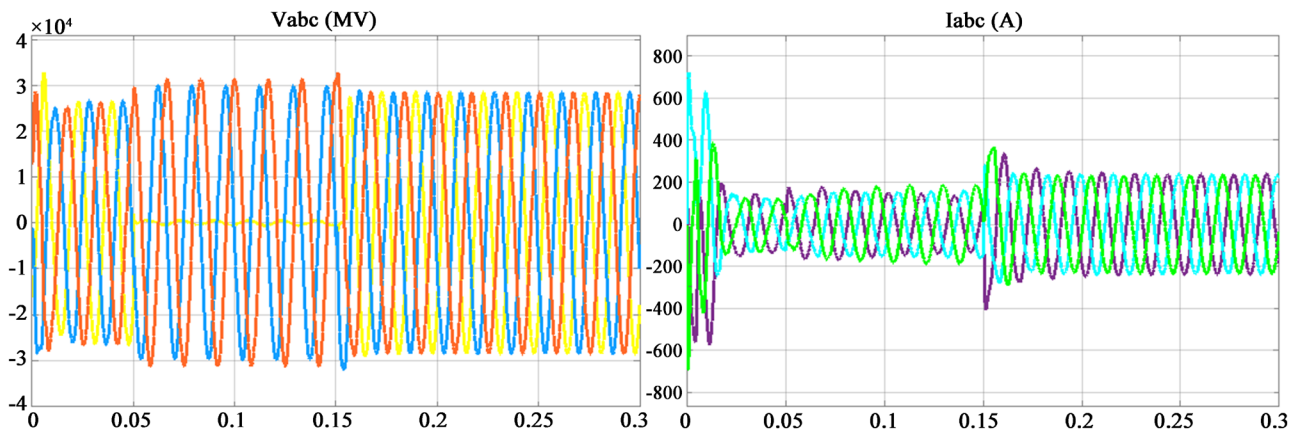


Figure 16. Variation of voltages and currents of a single-phase short-circuited network with RPI.

A single-phase short circuit of 0.2 ms duration in the presence of the RPI controller gives rise to a transient of 0.11 ms duration. **Table 7** shows the evolution of the network parameters in the presence of this fault.

We note in this table that a single-phase short-circuit in a network in the presence of the RPI controller causes current fluctuations with damped amplitudes and increasingly lower than the rated current.

4.2.6. Two-Phase Short-Circuit in the Presence of the RPI

The short-circuit administered at this level is a short-circuit between phase and phase, we have always administered it at the same period $t = 0.05$ ms and for the same 0.2 ms fault duration the observed behavior is as follows: (**Figure 17**).

- Visualization of voltages and current in the presence of an RPI

A two-phase short-circuit lasting 0.2 ms in the presence of the RPI controller gives rise to a transient regime lasting 0.125 ms. **Table 8** provides information

Table 7. Variation of network quantities in single-phase short-circuit with RPI.

STATE OF THE NETWORK AT FAULT WITH CONTROLLER						
Nature of the defect		Short-circuit single-phase current				
Type of controller	Sizes	Before defect	In the presence of the defect	Td (ms)	Error	Relative error in %
RPI 30P15	V (KV)	500	350	0.2	150	30
	I (KA)	2.8	0.26		2.54	90.71

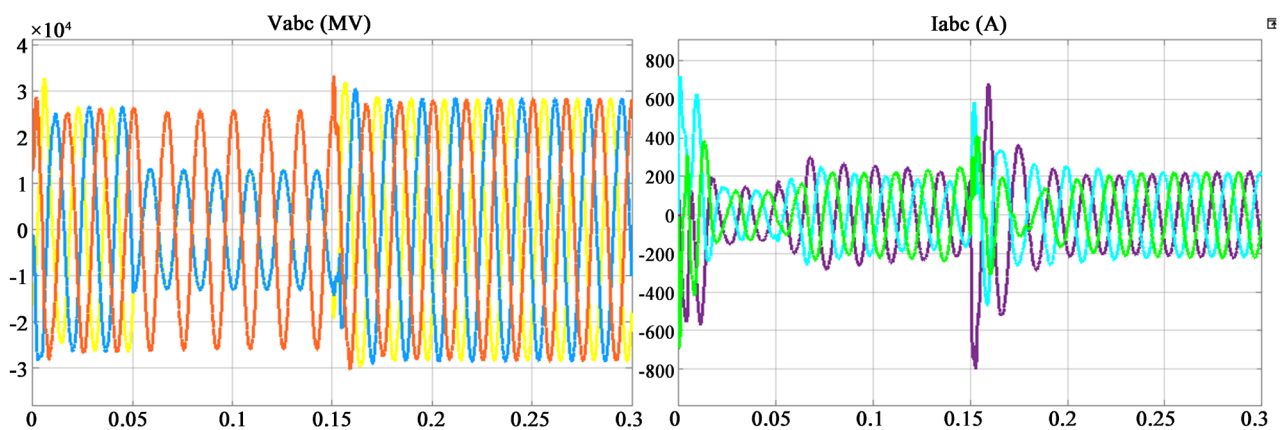


Figure 17. Variation of voltages and currents of a two-phase short-circuited network with UPFC.

Table 8. Variation of the two-phase short-circuit network quantities with RPI.

STATE OF THE NETWORK AT FAULT WITH CONTROLLER						
Nature of the defect		Two-phase short-circuit				
Type of controller	Sizes	Before defect	In the presence of the defect	Td (ms)	Error	Relative error in %
RPI 30P15	V (KV)	500	275	0.2	225	45
	I (KA)	2.8	0.658		2.142	76.5

on the evolution of the network parameters in the presence of this fault.

4.2.7. Breaking of a Phase in the Presence of RPI

In this part, we have made the same considerations for the time of the beginning of the fault as for its duration. The loss of one phase of the line in the presence of a controller can generate the phenomena observed below: (Figure 18).

- Visualization of voltages and currents in the presence of an RPI

Once again we can appreciate the juicy contribution of the RPI controller in improving network performance as shown in Table 9.

5. Comparative Study

In this part of the work, we will make a comparative study of the results obtained with a view to highlighting the assets or area of therapeutic competence of each technology. This analysis will be done in the form of a summary Table 10.

5.1. Short Circuit Fault

We notice in this table that a single-phase short-circuit in a network in the presence of the UPFC controller is characterized by a strong increase of the current which in certain cases, can go until exceeding the nominal current of the line whereas in the presence of the RPI controller this current tends to become increasingly lower than the nominal current. At the same time, at the level of the voltages, we observe rather the opposite facts, forcing us to say that the UPFC

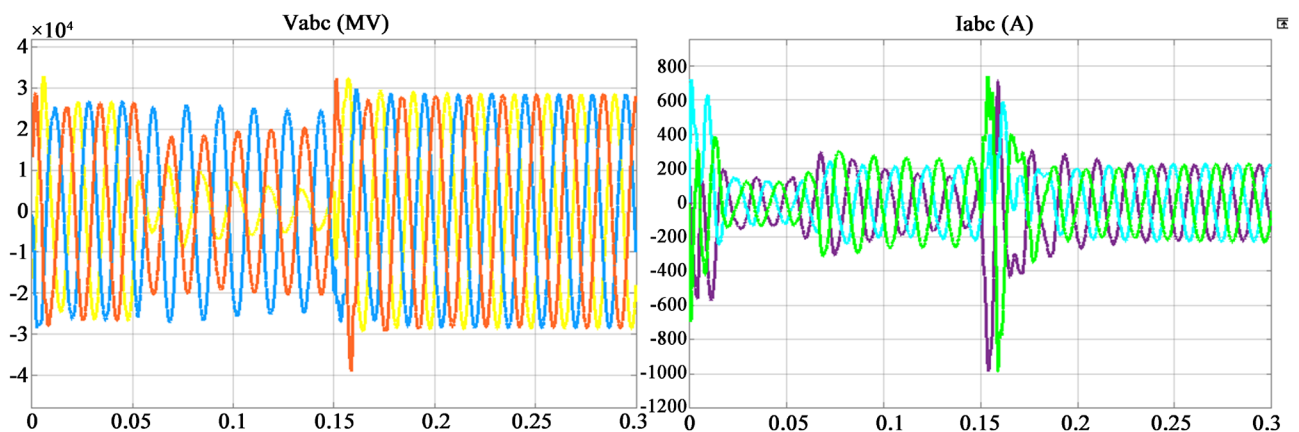


Figure 18. Variation of voltages and currents of a network with a phase deficit with RPI.

Table 9. Variation of the quantities of the network in phase failure with RPI.

STATE OF THE NETWORK AT FAULT WITH CONTROLLER						
Nature of the defect		Two-phase short-circuit				
Type of controller	Sizes	Before defect	In the presence of the defect	Td (ms)	Error	Relative error in %
RPI 30P15	V (KV)	500	306		194	38.8
	I (KA)	2.8	0.66	0.2	2.14	76.42

Table 10. Summary of the single-phase short-circuit network with regulator.

STATE OF THE NETWORK AT FAULT WITH CONTROLLER									
Nature of the defect		Short-circuit single-phase current					Two-phase short-circuit		
Type of controller	Sizes	Before defect	Td (ms)	In the presence of the defect	Relative error	Relative error In %	In the presence of the defect	Error	Erreur relative en %
UPFC	V (KV)	500		450	50	10	175	325	65
	I (KA)	2.8		2.4	0.4	14.28	1.63	1.17	41.78
RPI 30P15	V (KV)	500	0.2	350	150	30	275	225	45
	I (KA)	2.8		0.26	2.54	90.71	0.658	2.142	76.5

Table 11. Network summary with break of a phase with regulator.

STATE OF THE NETWORK AT FAULT WITH CONTROLLER						
Nature of the defect			Rupture of a phase			
Type of controller	Sizes	Before defect	In the presence of the defect	Td (ms)	Relative error	Relative error In %
UPFC	V (KV)	500	230		270	54
	I (KA)	2.8	0.9		1.9	90
RPI 30P15	V (KV)	500	306	0.2	194	38.8
	I (KA)	2.8	0.66		2.14	76.42

favors a good maintenance of the profile of the voltage plane rather than the RPI. We therefore have a voltage deficit of 10% for a network with UPFC rather than 30% for the network with RPI.

Also we notice in this table that a two-phase short circuit in a network in the presence of the UPFC controller is characterized by two current transients while the presence of the RPI controller gives rise to a single transient. We therefore have a voltage deficit of 65% for a network with UPFC rather than 45% for the network with RPI.

5.2. Breaking a Phase

We can see here that the loss of one phase negatively impacts all three phases of the network, both in the presence of a UPFC controller and an RPI controller. During this period, small differences can be seen. The network with UPFC is subtracted from 54% of its nominal voltage while the one with RPI is only debited from 38.8% of its voltage which explains in a certain way the flexibility of the RPI controller in the repair of the loads compared to the UPFC controller. (Table 11)

6. Conclusion

The current state of operation of the electricity networks is marked by constraints due to overloading, voltage drops, and the situation is further aggravated in the case of short circuits. The consequences are characterized by an insuffi-

cient level of service quality and high operating costs, due to the use of thermal generation and load shedding in case of incident. In order to optimize the operation of electrical transmission networks, we proposed to improve the operating conditions of the networks by two optimal control devices, namely the UPFC controller on the one hand and RPI on the other hand. In order to better understand the problem and to reach our objective, we have first presented the two technologies highlighted in order to understand their specificity. Subsequently, the feasibility and efficiency of the two controllers have been highlighted from a sample of results, obtained by simulating the prototype of a two-source transmission line, associated with a load. The results obtained show that the UPFC controller is effective in maintaining the voltage of the network and in repairing the load between the different phases. This last one presents weaknesses in front of a certain peak of the short-circuit fault, at this level the RPI30P15 controller showed itself more dynamic and even more adapted to this type of contingency. The UPFC can be considered here as an excellent support for maintaining the voltage of a disturbed network while the RPI can take the prize of excellent support for maintaining the network current. For future work, since power is dynamic, it will be appropriate to model an FPGA-driven RPI30P15 to better regulate power in electrical networks.

Conflicts of Interest

The authors declare no conflicts of interest regarding the publication of this paper.

References

- [1] Lemay, J., Brochu, J. and Beaugard, F. (2000) Interphase Power Controllers: The FACTS Family Is Growing.
- [2] Messalti, S. (2004) Evaluation of the Transient Stability of Electro-Energetic Systems by Neural Networks. Thesis, Faculty of Engineering Sciences, Department of Electrical Engineering, The University of Setif, Setif.
- [3] Brochu, J. (1996) Les Régulateurs de puissance interphases en régime établi.
- [4] Alkhatib, H. (2008) Study of Stability to Small Disturbances in Large Electrical Networks Optimization of Regulation by a Meta Heuristic Method. PhD Thesis, universite Paul Cezanne D'aix-Marseille Faculty of Sciences and Techniques.
- [5] CIGRE Task Force 38.02.17 (1999) Advanced Angle Stability Controls, a Technical Brochure for International Conference on Large High Voltage Electric Systems (CIGRE), December 1999.
- [6] Messalti, S. (2004) Evaluation De La Stabilité Transitoire Des Systèmes Électro énergétiques Par Les réseaux De Neurones (Evaluation of the Transient Stability of Electro-Energetic Systems by Neural Networks). Faculty of Engineering Sciences, Department of Electrical Engineering, The University of Setif, Setif.
- [7] Brochu, J. (1999) Interphase Power Controllers. Polytechnic International Press, Montreal.
- [8] Montreio, A.M. (2005) Study of Short-Circuit Current Limiting Devices (Interphase Power Controller). VII, 115 p.

- [9] Lu, W. (2009) Optimal Load Shedding for the Prevention of Large Power Outages. Doctor De L'institut Polytechnique De Grenoble July 6.
- [10] Mandeng, J., Kom, C. and Mbihi, J. (2017) Design of an Automated Dual IPCs 240 System for Asymmetric Power Flow Compensation in an AC Electric Network. *Transactions on Electrical Engineering*, **6**, 32-39.
<https://doi.org/10.14311/TEE.2017.2.032>
- [11] Brochu, J., Beauregard, F., Lemay, J., Pelletier, P. and Marceau, R.J. (1997) Steady-State Analysis of Power Flow Controllers Using the Power Controller Plane. *IEEE Transactions on Power Delivery*, **14**, 1024-1031.
- [12] Wildi, T. and Sybille, G. (2007) Electrical Engineering. 4th Edition. Bruxelles, Sreetthe Minimes University.
- [13] Crappe, M. (2003) Stabilité et sauvegarde des réseaux d'énergie électrique. Bermes Science Publication, Lavoisier.
- [14] Joseph, K.K., Léandre, N.N., Charles Hubert, K. and Essiane Salomé, N. (2020) Contribution to the Optimization of the Transient Stability of an Electric Power Transmission Network Using a UPFC Stabilizer Controlled by a Three-Stage Inverter. *World Journal of Engineering and Technology*, **8**, 675-688.
- [15] Brogan, W.L., *et al.* (2000) Control Systems. The Electric Engineering Handbook. CRC Press, Boca Raton.
- [16] Hennebel, M. (2009) Valuation of System Services on an Electricity Transmission Network in a Competitive Environment. PhD Thesis, Paris University, Paris.
- [17] Gholipour, S.E. (2003) UPFC's Contribution to Improving the Transient Stability of Electrical Networks. Doctoral Thesis, Faculty of Sciences & Techniques, Henri Poincaré University, Nancy.